Soluble EP2 neutralizes prostaglandin E_2–induced cell signaling and inhibits osteolytic tumor growth

Tetsuyuki Takahashi, Hisanori Uehara, Yoshimi Bando, and Keisuke Izumi

Department of Molecular and Environmental Pathology, Institute of Health Biosciences, The University of Tokushima Graduate School, Tokushima, Japan

Abstract

Prostaglandin E_2 (PGE_2) plays a key role in osteolytic bone metastasis as well as roles in inflammation, cell growth, and tumor development. PGE_2 exerts its effects by binding and activating E-prostanoid receptor (EP). In this study, we propose a new approach for blocking EP-mediated cell signaling using a soluble chimeric EP2 fragment. Mammalian expression vectors encoding several human EP2 cDNAs were introduced into 293 cells and the culture medium was tested for their function as a decoy receptor for PGE_2. PGE_2 binding assays revealed that culture medium containing the second extracellular region of EP2 (FuEP2/Ex2) had binding activity. FuEP2/Ex2 neutralized PGE_2-induced cyclic AMP production, cyclic AMP–responsive element binding protein phosphorylation, and subsequent induction of cyclooxygenase-2, interleukin (IL)-1β, and IL-6 mRNAs. In human osteoblasts, this culture medium neutralized the induction of receptor activator of nuclear factor-κB ligand mRNA. A stable transfectant expressing FuEP2/Ex2 was established from human prostate cancer PC-3 cells (PC3-FuEP2/Ex2). PC3-FuEP2/Ex2 cells grew at similar rates to vector control cells under normal culture conditions, although PGE_2-induced growth stimulation was suppressed. Intraosseous injection of PC3-FuEP2/Ex2 cells into the tibia of athymic nude mice revealed that the degrees of tumor growth and osteolysis were decreased compared with control cell-injected mice, with decreased osteoclasts and increased apoptotic cells. Furthermore, the cyclooxygenase-2, IL-1β, and IL-6 mRNA levels were reduced in the tumor lesions. These data suggest that FuEP2/Ex2 is useful for treating osteolytic bone metastasis and cancers that depend on EP signaling for their growth and development. [Mol Cancer Ther 2008;7(9):2807–16]

Introduction

Prostaglandins are autacoid substrates produced from arachidonic acid and play important roles in physiologic homeostasis as paracrine factors. Especially, prostaglandin E_2 (PGE_2) is closely associated with inflammation, cell growth, tumor development, and tumor metastasis (1). In addition, PGE_2 is a key molecule for bone metabolism. PGE_2 is produced in bone by osteoblasts and acts as a stimulator of bone resorption. This effect is closely associated with osteolytic cancer bone metastasis, which involves in bone destruction (2). This knowledge is further supported by reports that administration of cyclooxygenase (COX) inhibitors suppresses the bone metastasis of breast and prostate cancer cells (3, 4).

Prostaglandins exert their effect by binding to specific cell surface receptors designated prostanoid receptors. The receptors for PGE_2 are known as E-prostanoid receptors (EP) and are composed of four subtypes (EP1-EP4; ref. 5). All the EPs are seven-transmembrane domain G protein-coupled receptors and are classified into three types based on their signal transduction features. Activation of EP1 results in elevation of intracellular calcium. EP2 and EP4 signaling elicits cyclic AMP (cAMP) generation, whereas EP3 signaling exerts the opposite effect (6–9). The increased cellular cAMP level induced by EP2 and EP4 causes activation of protein kinase A and phosphatidylinositol 3-kinase. Protein kinase A mainly catalyzes phosphorylation of cAMP-responsive element binding protein (CREB), an inducible transcription factor that binds to cAMP response elements and is related to cellular responses of inflammation and cancer progression (10). Indeed, EP1- and EP4-deficient mice show resistance toward azoxymethane-induced colon carcinogenesis, whereas EP2-deficient *APC*-knockout mice exhibit decreases in the number and size of intestinal polyps (11–13). Oral administration of specific antagonists for several EPs also inhibits colon carcinogenesis and experimental metastasis (14–16). These reports strongly suggest that PGE_2-mediated EP signaling is closely related to a wide range of cancer stages, including carcinogenesis, tumor development, and the various types of metastasis.

EP signaling is closely involved with bone metastasis. Interactions between cancer cells and the bone microenvironment are thought to represent a major stage in bone metastasis signaling. This signaling plays a pivotal role in osteolysis by inducing the differentiation of monocytes/macrophages into osteoclasts. PGE_2 mainly binds to EP4 in osteoblasts and activates cellular cAMP followed by up-regulation of receptor activator of nuclear factor-κB ligand

Received 2/11/08; revised 5/22/08; accepted 6/9/08.

Grant support: Ministry of Education, Science, Sports and Culture of Japan Grant-in-Aid for Scientific Research (C) 18590373 (H. Uehara).

The costs of publication of this article were defrayed in part by the payment of page charges. This article must therefore be hereby marked *advertisement* in accordance with 18 U.S.C. Section 1734 solely to indicate this fact.

Requests for reprints: Hisanori Uehara, Department of Molecular and Environmental Pathology, Institute of Health Biosciences, The University of Tokushima Graduate School, 3-18-15, Kuramoto-cho, Tokushima-shi, Tokushima, Japan. Phone: 81-88-633-7066; Fax: 81-88-633-7067. E-mail: uehara@basic.med.tokushima-u.ac.jp

doi:10.1158/1535-7163.MCT-08-0153

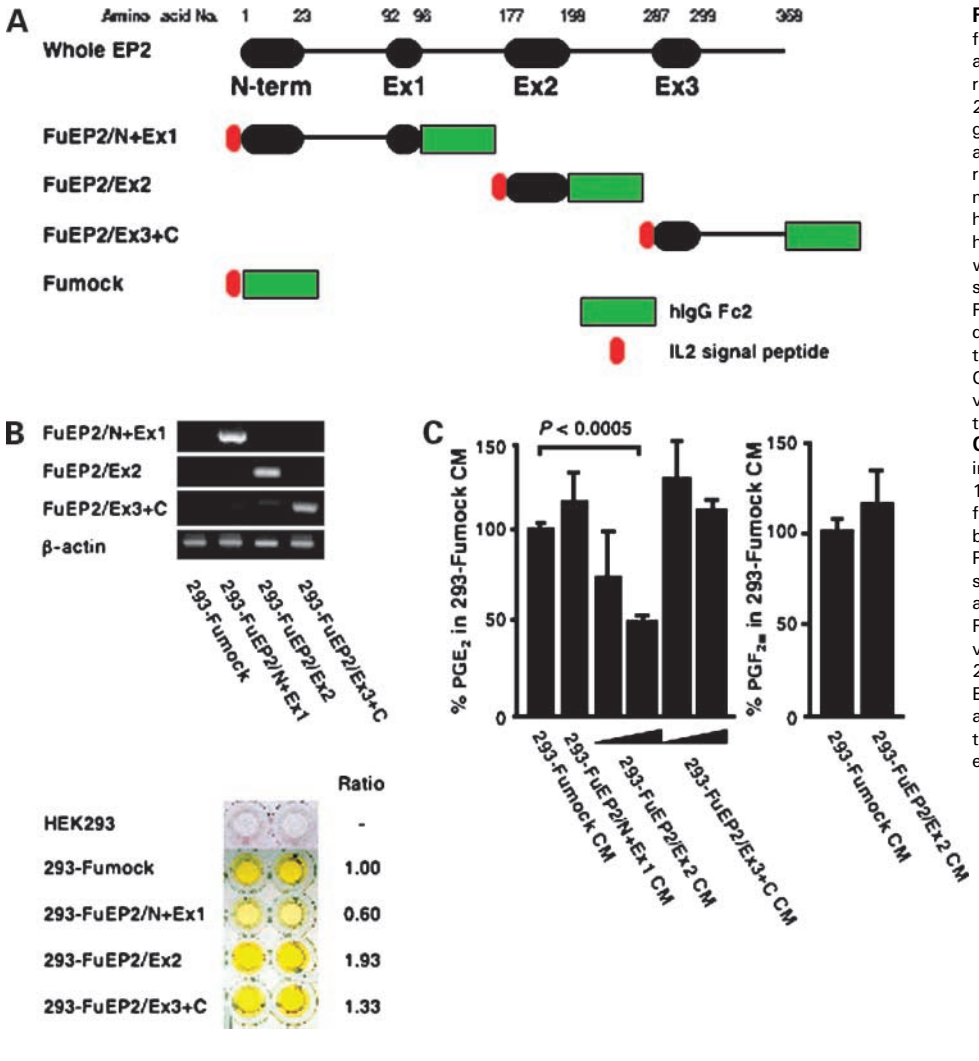

Figure 1. IL2ss/hIgG-fused hEP2 fragments and their PGE_2-capturing activities. **A,** hEP2 has four extracellular regions (1-23, 92-96, 177-198, and 287-299; *filled ellipses*). All fragments generated in this study had IL2ss fused at the NH_2 terminus and the hIgG Fc2 region fused at the COOH terminus. **B,** mammalian expression vectors pFUSE-hFc2, pFUSE-hEP2/N + Ex1, pFUSE-hEP2/Ex2, and pFUSE-hEP2/Ex3 + C were introduced into HEK293 cells and stable transfectants were established. RT-PCR and ELISA for hIgG were conducted using RNA and CM from these transfectants. The relative ratios of each CM were calculated by using A_{450} values of ELISA, when the value for the 293-Fumock CM was set at 1.00. **C,** CM from their transfectants was incubated with 250 pg/mL PGE_2 or 125 pg/mL $PGF_{2\alpha}$ for 30 min and hEP2 fragments in the CM were pulled down by protein G-agarose. The remaining PGE_2 or $PGF_{2\alpha}$ levels in the collected supernatants were assayed by EIA. The amount of PGE_2 or $PGF_{2\alpha}$ in 293-Fumock CM was assigned as 100% value and the relative percentages in 293-FuEP2/N + Ex1 CM, 293-FuEP2/Ex2 CM, and 293-FuEP2/Ex3 + C CM are shown. *Columns,* mean percentages (n = 6) of three independent experiments; *bars,* SD.

(RANKL; refs. 17, 18). The increased RANKL consequently associates with RANK in monocytes/macrophages and enhances their differentiation into osteoclasts (19). This event frequently occurs during bone resorption, and inhibition of EP signaling by genetic disruption of EPs or administration of COX-2-specific inhibitors and EP4-specific antagonists result in decreased degrees of bone resorption and cancer bone metastasis *in vivo* (20–22).

In the present report, we propose a novel approach for antagonizing PGE_2-mediated EP signaling by directly neutralizing PGE_2 using a soluble fragment of the EP2 receptor. We generated several EP2 fragments by fusing the interleukin (IL)-2 signal peptide at the NH_2 terminus and the human IgG2 (hIgG2) Fc region at the COOH terminus. These fragments were examined for their expression profiles, PGE_2-capturing activities, and neutralizing effects for PGE_2-induced cell signaling in human prostate cancer PC-3 cells and primary human osteoblasts. We found that the fragment containing the second extracellular region of EP2 functions as a scavenger for PGE_2 and neutralizes PGE_2-induced cell signaling. We further evaluated the inhibitory effect of this fragment on the growth of prostate cancer cells using a xenograft model in nude mice.

Materials and Methods

Cell Cultures and Animals

Human embryonic kidney 293 cells and human prostate adenocarcinoma PC-3 cells (purchased from Human Science Research Resources Bank) were maintained in MEM supplemented with 10% fetal bovine serum (FBS), 100 units/mL penicillin G, and 0.1 mg/mL streptomycin sulfate. Primary cultured human osteoblasts were maintained in OBM medium (Lonza). PC-3 cells were reported previously to be EP2 and EP4 positive (23). Four-week-old male athymic nude mice were purchased from Charles River Japan. Mice were housed and maintained under specific pathogen-free conditions. Experiments were done

according to the Guideline for the Care and Use of Laboratory Animals of the University of Tokushima School of Medicine and were approved by the Animal Committee.

Construction of Mammalian Expression Vectors

cDNAs containing the complete coding sequence of human EP2 (hEP2) were synthesized from total RNA isolated from 24 h serum-starved PC-3 cells using SuperScript II reverse transcriptase and random hexamers (Invitrogen). The reactions were conducted at 42°C for 60 min, after which the temperature was increased to 72°C for 15 min. The total cDNAs were then amplified by PCR following a thermocycling program of 94°C for 10 min for initial denaturation, 40 cycles of 94°C for 30 s, 55°C for 1 min, and 72°C for 1 min for amplification, and a final extension at 72°C for 10 min. The primers used in this study are listed in Supplementary Table S1.[1] All the PCR products were digested with *Eco*RI and *Bgl*II and subcloned into the pFUSE-hFc2 (IL2ss) vector (Invivogen). The constructs made by the above procedure were designated pFUSE-hEP2/N+Ex1, pFUSE-hEP2/Ex2, and pFUSE-hEP2/Ex3+C. Their successful constructions were confirmed by direct sequencing using an ABI PRISM 3100-Avant Genetic Analyzer (Applied Biosystems). The structures of the fusion proteins are shown in Fig. 1A.

Stable Transfection

Cells were stably transfected using a cationic liposome-based method. Expression vectors (13.6 μg per 4×10^5 cells) were mixed with 40.8 μL TransFast transfection reagent (Promega) in 680 μL MEM containing 10% FBS and incubated at room temperature for 15 min. The mixtures were then added to six-well plates (4×10^5 cells per well) and incubated for 2 h. Next, the mixtures were removed and further incubated with 1.2 mL complete culture medium (CM). The cells were reseeded at 4×10^5 and incubated in the presence of 2 mg zeocin (Invivogen). Exposure to zeocin was repeated every 3 days. After selection for zeocin-resistant cells for 2 weeks, the stable transfectants obtained were maintained in complete CM containing 100 μg/mL zeocin. These transfectants (4×10^5) were seeded onto six-well plates and preincubated at 37°C for 18 h, and the medium was replaced to 1.2 mL MEM containing 2% FBS. After incubation for 48 h, the CM was collected and used for the following experiments.

Detection of mRNA and Protein Expression Levels

Total RNAs from transfectants or human osteoblasts were isolated using an RNeasy Mini kit (Qiagen). Aliquots of these total RNAs (2 μg/sample) were subjected to reverse-transcription PCR (RT-PCR) under the same conditions used for preparing the hEP2 cDNAs. β-Actin was amplified as an internal standard. In this amplification, the forward primer, IL2ss PCR-F, was expression vector-dependent and its sequence was 5′-ATGTACAGGATGCAACTC-3′. In transfectants, CM from the transfectants was also used for the detection of secreted hIgG Fc-fusion proteins derived from expression vectors. A hIgG ELISA quantification kit (Bethyl Laboratories) was employed for the detection.

PGE_2-Capturing Activity Assay

We tested whether the CM could capture PGE_2. First, the collected CM was incubated with 250 pg/mL PGE_2 (Cayman Chemical) at 37°C for 30 min. Next, the samples were pulled down with a protein G-agarose conjugate (Calbiochem) by rotating for 30 min at room temperature and the supernatants were collected as samples. The concentrations of PGE_2 remaining in the samples were determined using a PGE_2 Express Enzyme Immunoassay (EIA) kit (Cayman Chemical). To check the specificity, the totally same procedure by using $PGF_{2\alpha}$ and Prostaglandin $F_{2\alpha}$ EIA kit (Cayman Chemical) was also conducted. In this method, CM was incubated with 125 pg/mL $PGF_{2\alpha}$.

Western Blot Analysis

The effects of 293-FuEP2/Ex2 CM on CREB phosphorylation were analyzed by Western blotting. PC-3 cells (4×10^5) were seeded onto six-well plates, preincubated at 37°C for 18 h, and then starved for 24 h by incubation in 1 mL serum-free MEM. Next, the cells were treated with 2 or 20 μmol/L PGE_2-containing 293-Fumock or 293-FuEP2/Ex2 CM (final concentrations of FBS and PGE_2 were 1%, 1 μmol/L, and 10 μmol/L, respectively) for 5 min. The cells were then lysed with radioimmunoprecipitation assay buffer [50 mmol/L Tris-HCl (pH 7.5), 150 mmol/L NaCl, 1% NP-40, 0.5% sodium deoxycholate, 0.1% SDS, 1 mmol/L DTT, and 1 mmol/L phenylmethylsulfonyl fluoride] and the protein concentrations of the samples were quantified using a DC Protein Assay kit (Bio-Rad). Subsequently, aliquots (30 μg protein) were subjected to SDS-PAGE (10.5% gel) and transferred to polyvinylidene difluoride membranes. Rabbit antibodies against phosphorylated CREB (S133; R&D Systems), CREB, and actin (Sigma) were used as the primary antibodies. Goat anti-rabbit IgG-horseradish peroxidase (Invitrogen) was employed as the secondary antibody. The dilution rates were as follows: anti-phosphorylated CREB (1:1,000), anti-CREB (1:500), anti-actin (1:5,000), and anti-rabbit IgG-horseradish peroxidase (1:150,000). An Immobilon Western horseradish peroxidase substrate (Millipore) was applied to detect the signals.

Semiquantitative RT-PCR

The mRNA levels of COX-2, IL-1β, and IL-6 in PC-3 cells, RANKL in human primary osteoblasts, and β-actin in both cell types were analyzed by semiquantitative RT-PCR. PC-3 cells (2×10^5) and human primary osteoblasts (2×10^5) were seeded onto six-well plates, preincubated at 37°C for 18 h, and then starved for 24 h by incubation in 1 mL serum-free MEM. Next, an equal volume of 293-Fumock or 293-FuEP2/Ex2 CM was added to each well in the presence of 2 or 20 μmol/L PGE_2 (final concentrations of FBS and PGE_2 were 1%, 1 μmol/L, and 10 μmol/L, respectively) and the cells were stimulated for 4 h at 37°C. Total RNAs were isolated using a RNeasy Mini kit and subjected to RT-PCR

[1] Supplementary material for this article is available at Molecular Cancer Therapeutics Online (http://mct.aacrjournals.org/).

under the same conditions used for preparing the hEP2 cDNAs, except for the numbers of amplification cycles (COX-2, IL-1β, IL-6, and β-actin: 23 cycles and RANKL: 35 cycles). The RT-PCR products were separated by 1.5% agarose gel electrophoresis and visualized with an UV transilluminator. The primers used in this experiment are listed in Supplementary Table S1.[1]

Proliferation Assays

PC3-Fumock and PC3-FuEP2/Ex2 cells (5×10^3) were plated on 96-well microplates and preincubated at 37°C for 18 h. Next, the CM was replaced with 100 μL fresh complete medium and the numbers of viable cells after incubation for 24, 48, and 72 h were determined by the MTT method. A colony formation assay was conducted in parallel. Three hundred PC3-Fumock or PC3-FuEP2/Ex2 cells were seeded onto six-well plates and incubated at 37°C for 10 days. The resulting colonies were fixed with methanol for 2 min, stained with Giemsa staining solution (Muto Pure Chemicals) for 20 min, and then counted under a microscope. The influence of PGE_2 on cell growth was also tested. PC3-Fumock and PC3-FuEP2/Ex2 cells (5×10^3) were plated on 96-well microplates and preincubated at 37°C for 18 h. Under serum-free conditions, the cells were then incubated with or without 1 and 10 μmol/L PGE_2 at 37°C for 24 h, and viable cells were determined by the MTT method.

Bone Metastasis Model in Nude Mice

Intratibial injections of PC3-Fumock and PC3-FuEP2/Ex2 cells were done as described previously (24). PC3-Fumock or PC3-FuEP2/Ex2 cells (5×10^5 per mice) were intraosseally injected into the proximal tibia to the tuberositas tibia. After 9 weeks of observation, the hind limbs of the mice were analyzed by X-ray radiography. Subsequently, the mice were sacrificed and the tumor incidence, leg weight (excised at the knee joint), and incidence of intraabdominal lymph node metastases were recorded. In both groups, an area of tumor tissue was collected and total RNA was isolated. Total RNAs (4 μg/reaction) were subjected to semiquantitative RT-PCR under the same conditions used for preparing the hEP2 cDNA.

Histologic Analyses

After measuring their weights, the legs were fixed in 10% phosphate-buffered formaldehyde at room temperature for 24 h, washed with PBS for 30 min, and decalcified with 10% EDTA (pH 7.4) at 4°C for 14 days. The tissues were then embedded in paraffin and sectioned at 4 to 6 μm. Detection of osteoclasts was conducted by tartrate-resistant acid phosphatase (TRAP) staining, which is specific for osteoclasts. Sections were stained with TRAP staining solution [5 mg naphthol AS-MX phosphate and 30 mg Fast Red Violet LB salt (Sigma) in 50 mL TRAP buffer (50 mmol/L sodium tartrate and 45 mmol/L sodium acetate)] and the

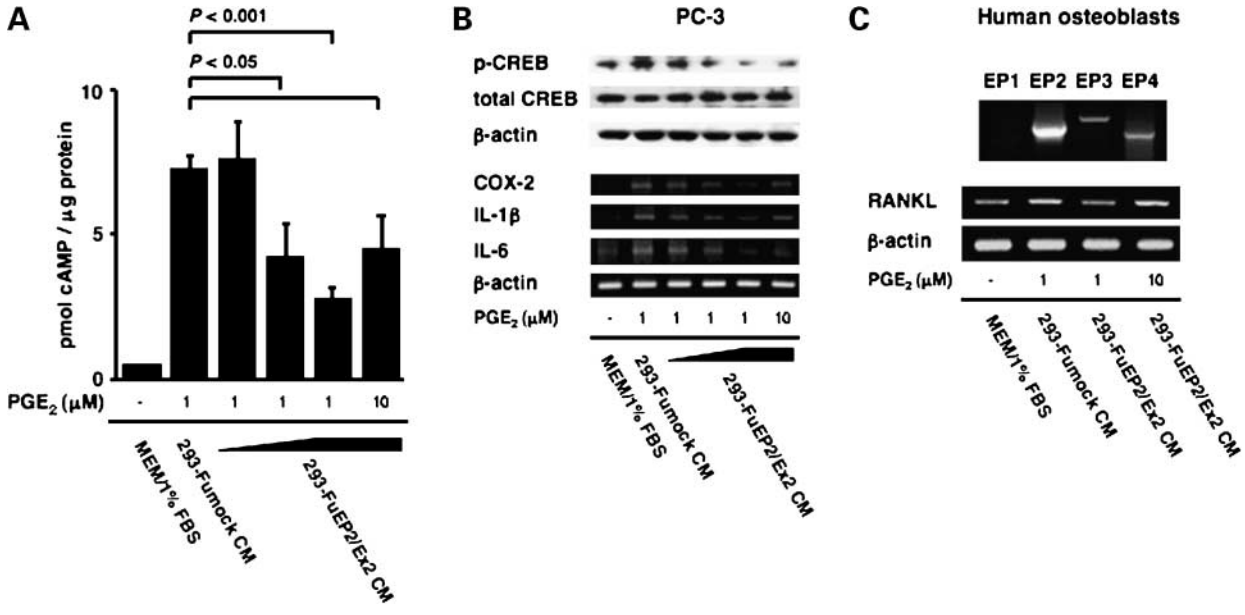

Figure 2. Neutralizing effects of 293-FuEP2/Ex2 CM on PGE_2-induced cell signaling. **A,** PC-3 cells were stimulated with 1 or 10 μmol/L PGE_2 for 5 min in the presence of 1% FBS. The amounts of intracellular cAMP were determined by EIA. The doses of 293-FuEP2/Ex2 CM were 1-, 2-, and 3-fold higher than the dose of 293-Fumock CM. *Columns,* mean ($n = 4$) of two independent experiments; *bars,* SD. **B,** PC-3 cells were stimulated with 1 or 10 μmol/L PGE_2 for 5 min (Western blot analyses) or 4 h (semiquantitative RT-PCR) in the presence of 1% FBS. The levels of phosphorylated CREB and total CREB were determined by Western blot analysis. The levels of COX-2, IL-1β, and IL-6 mRNAs were determined by semiquantitative RT-PCR. The doses of 293-FuEP2/Ex2 CM were 1-, 2-, and 3-fold higher than the dose of 293-Fumock CM. Representative of three separate experiments. **C,** expression of EP receptors in human primary osteoblasts was examined by RT-PCR. The sizes of the amplified PCR products for EP1, EP2, EP3, and EP4 are 603, 594, 681, and 552 bp, respectively. Next, the cells were stimulated with 1 μmol/L PGE_2 for 4 h in presence of 1% FBS. The levels of RANKL mRNA were determined by semiquantitative RT-PCR. The dose of 293-FuEP2/Ex2 CM was 3-fold higher than the dose of 293-Fumock CM. The levels of β-actin mRNA were employed as an internal loading control. Representative of two separate experiments.

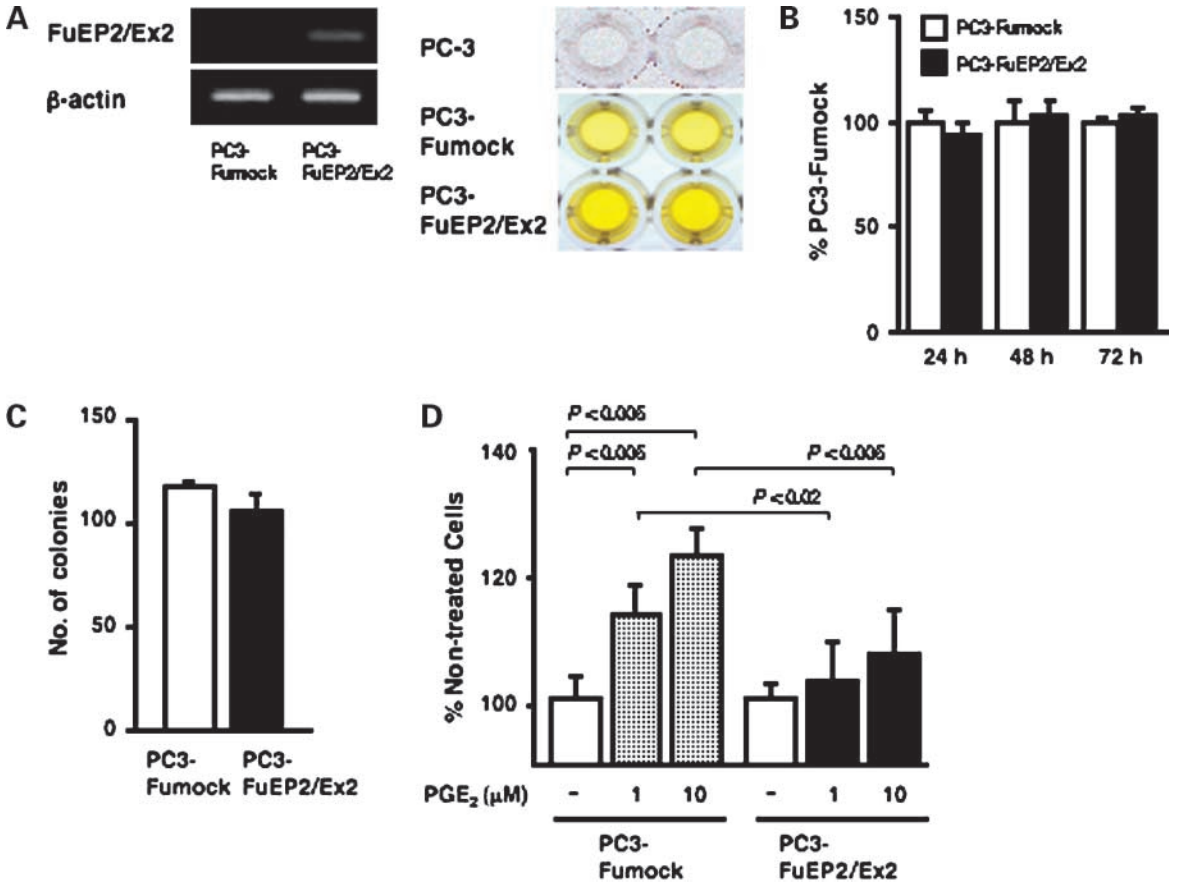

Figure 3. Characteristics of PC3-FuEP2/Ex2. **A,** mammalian expression vectors pFUSE-hFc2 and pFUSE-hEP2/Ex2 were introduced into PC-3 cells and stable transfectants were established. Successful mRNA expression and protein secretion of the fragments into the CM were confirmed by RT-PCR (*left*) and ELISA (*right*) for hIgG. **B,** PC3-Fumock and PC3-FuEP2/Ex2 cells were incubated in complete medium for 24, 48, and 72 h and cell proliferation was measured by the MTT assay. The A_{550} value for PC3-Fumock cells was assigned as 100% and the relative percentages of PC3-FuEP2/Ex2 cells are shown. *Columns,* mean percentages ($n = 6$) of three independent experiments; *bars,* SD. **C,** PC3-Fumock and PC3-FuEP2/Ex2 cells were incubated in complete medium for 10 d and cell proliferation was measured by a colony formation assay. *Columns,* mean numbers of colonies ($n = 3$) of three independent experiments; *bars,* SD. **D,** PC3-Fumock and PC3-FuEP2/Ex2 cells were treated with 1 and 10 μmol/L PGE_2 in serum-free medium for 24 h and cell proliferation was measured by the MTT assay. The A_{550} values for nontreated cells were assigned as 100% and the relative percentages of PGE_2-treated cells are shown. *Columns,* mean percentages ($n = 6$) of three independent experiments; *bars,* SD.

numbers of stained osteoclasts were counted under a microscope. The osteoclast density was calculated based on the number of TRAP-positive cells per length of bone surface contacting the tumor region. Expression of Ki-67 and cleavage of caspase-3 were also detected by immunohistochemical analyses. A monoclonal mouse anti-Ki-67 antibody (DakoCytomation) and polyclonal rabbit anti-cleaved caspase-3 antibody (Cell Signaling Technology) were used as the primary antibodies at dilutions of 1:50 and 1:200, respectively. Before probing with the primary antibodies, the antigens were retrieved by autoclaving the sections in 0.01 mol/L citrate buffer (pH 6.0) for 10 min. Visualization was completed using a ChemMate ENVISION kit/horseradish peroxidase (DakoCytomation). All sections were counterstained with Mayer's hematoxylin (Muto Pure Chemicals).

Statistical Analyses

A two-tailed Student's *t* test was employed for comparison of the PGE_2-capturing activity assays, cell growth assays, average hind limb weights, numbers of osteoclasts in bone, percentages of Ki-67-positive cells, and percentages of cleaved caspase-3-positive cells. The χ^2 test was used for comparisons of the incidences of lymph node metastases. In all cases, $P < 0.05$ was considered significant.

Results

Expression and Secretion of hEP2 Fragments

HEK293 cells were used to express and secrete of several IL2ss/IgG-fused hEP2 fragments. We tried to establish stable transfectants by selection with zeocin and expression checks were conducted. RT-PCR analyses revealed that all transfectants successfully expressed mRNAs encoding the individual hEP2 fragments (Fig. 1B). ELISA for hIgG showed that 293-Fumock, 293-FuEP2/N+Ex1, 293-FuEP2/Ex2, and 293-FuEP2/Ex3+C cells secreted hEP2 fragments into the CM, whereas no hIgG was detected in the CM from parent HEK293 cells (Fig. 1B). Comparisons of the secretion

levels based on the A_{450} values showed that the hIgG levels in the 293-FuEP2/N+Ex1, 293-FuEP2/Ex2, and 293-FuEP2/Ex3+C CM were 0.60-, 1.93-, and 1.33-fold when the value for the 293-Fumock CM was set at 1.00, respectively. The calculated fragment concentrations (using hIgG as a standard protein) were as follows: 293-Fumock, 49.8 ± 2.6 ng/mL; 293-FuEP2/N+Ex1, 14.1 ± 3.9 ng/mL; 293-FuEP2/Ex2, 132.2 ± 3.5 ng/mL; and 293-FuEP2/Ex3+C, 78.7 ± 115 ng/mL (data not shown).

Effects of hEP2 Fragments on PGE2-Capturing Activity

The PGE_2-capturing activities were assayed using the CM from 293-Fumock, 293-FuEP2/N+Ex1, 293-FuEP2/Ex2, and 293-FuEP2/Ex3+C cells. Samples were incubated with PGE_2, pulled down by protein G-agarose, and analyzed by EIA. The doses of the CM were corrected by the A_{450} values, and the CM from 293-FuEP2/Ex2 and 293-FuEP2/Ex3+C were set up as 1- and 2-fold dose groups relative to the 293-FuEP2/N+Ex1 CM, which recorded the lowest concentration of secreted fusion protein. (The meaning of 2-fold dose group is the 2-fold amount of fusion protein as nondiluted 293-FuEP2/N+Ex1 CM.) The remaining PGE_2 decreased dose-dependently in the 293-FuEP2/Ex2 CM groups. In particular, the 2-fold dose group showed a significant decrease in PGE_2 (48.6 ± 5.6%) compared with the 293-Fumock CM ($P < 0.0005$; Fig. 1C). The 293-FuEP2/Ex2 CM was also tested whether it occurs nonspecific and/or unexpected effect by $PGF_{2\alpha}$-capturing activity assay. This experiment showed that the 2-fold dose group of 293-FuEP2/Ex2 CM, which is significant effective in PGE_2-capturing activity assay, cannot decrease the remaining $PGF_{2\alpha}$ (Fig. 1C). To confirm these results, a cell-based binding assay using a biotinylated PGE_2 and Alexa 488-streptavidin in PC-3 cells was done and revealed the same trend (Supplementary Fig. S1).[1] However, when we tried to check the capturing activities of the corresponding fragments in other subtypes of EPs by establishing 293-FuEP1/Ex2, 293-FuEP3/Ex2, and 293-FuEP4/Ex2 cells, the levels of the fragments secreted into the CM were very low and below the detection limit of this assay (data not shown).

FuEP2/Ex2 CM Inhibits PGE_2-Induced Signal Transduction

To evaluate whether 293-FuEP2/Ex2 functions as a neutralizing agent for PGE_2, the effect of 293-FuEP2/Ex2 CM on PGE_2-induced signal transduction was examined by EIA for cAMP, Western blot analysis, and semiquantitative RT-PCR. We employed PC-3 cells to examine the effects on cAMP production, CREB phosphorylation, and induction of COX-2, IL-1β, and IL-6 mRNAs. The amounts of 293-FuEP2/Ex2 CM were set up as 1-, 2-, and 3-fold dose groups relative to the 293-Fumock CM. When treated with 293-FuEP2/Ex2 CM, the increase in cAMP production induced by 1 μmol/L PGE_2 was dose-dependently inhibited. In the 2- and 3-fold dose groups, the inhibition was significant ($P < 0.05$ in the 2-fold dose group and $P < 0.001$ in the 3-fold dose group; Fig. 2A). This inhibition was attenuated by excess amount (10 μmol/L) of PGE_2 (from 2.54 ± 0.60 to 4.28 ± 1.29 pmol/mg protein). Western blot analysis and semiquantitative RT-PCR revealed that the levels of phosphorylated CREB and COX-2, IL-1β, and IL-6 mRNAs were increased in PGE_2-treated cells compared with nontreated cells. In the 3-fold dose group of 293-FuEP2/Ex2 CM-treated cells, the level of phosphorylated CREB was clearly decreased (Fig. 2B). Furthermore, the COX-2, IL-1β, and IL-6 mRNA levels were dose-dependently attenuated in this group (Fig. 2B). These attenuations were also decreased by treatment of 10 μmol/L PGE_2. Human osteoblasts were used to test the inhibitory effect of 293-FuEP2/Ex2 CM on the induction of RANKL mRNA. In these cells, expression of EP2, EP3, and EP4 was detected and the level of RANKL mRNA was increased by

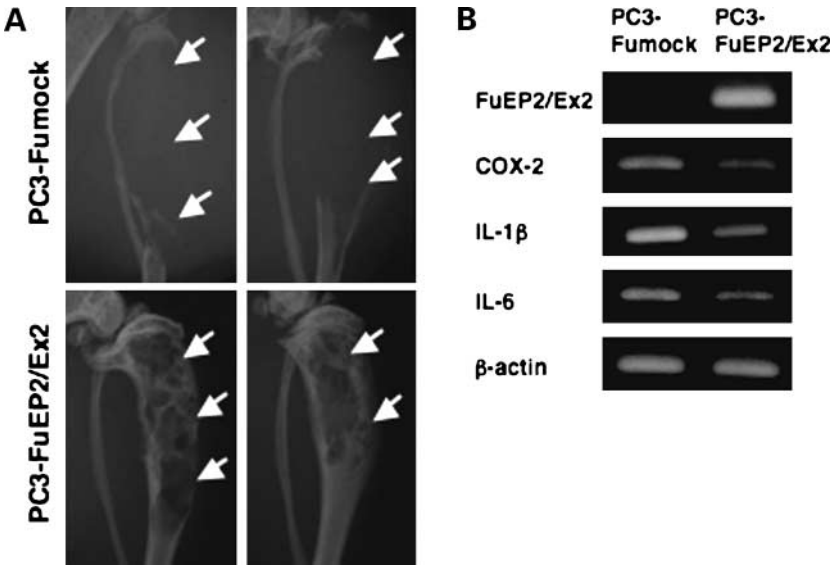

Figure 4. Effects of FuEP2/Ex2 on tumor growth in bone and expression of COX-2, IL-1β, and IL-6 mRNAs. **A,** representative X-ray radiographs of PC3-Fumock- or PC3-FuEP2/Ex2-injected mice at 9 wk after injection. *Arrowheads,* osteolytic lesion. **B,** using part of the tumor tissues at 9 wk after injection of PC3-Fumock or PC3-FuEP2/Ex2 cells, the COX-2, IL-1β, IL-6, and β-actin mRNA levels were analyzed by semiquantitative RT-PCR.

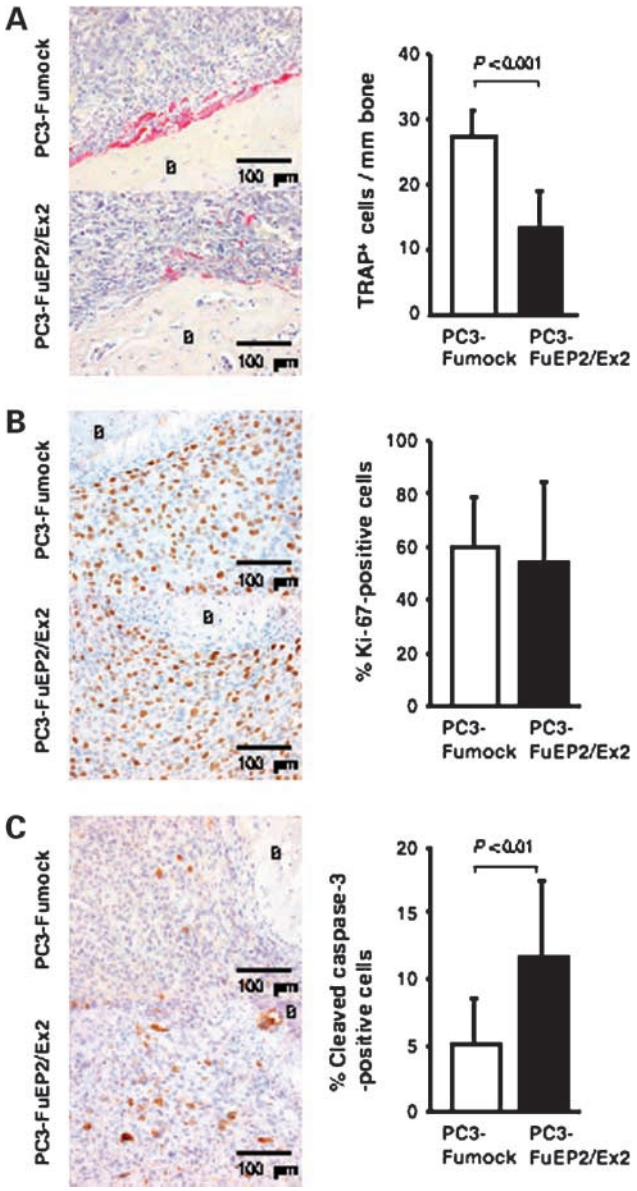

Figure 5. TRAP staining and immunohistochemical staining for Ki-67 antigen and cleaved caspase-3. At 9 wk after intratibial injection of PC3-Fumock or PC3-FuEP2/Ex2 cells into nude mice, the hind limbs were fixed in formaldehyde, embedded in paraffin, and sectioned. The sections were then subjected to TRAP staining (**A**) and immunohistochemical staining with an anti-Ki-67 antibody (**B**) or anti-cleaved caspase-3 antibody (**C**). Representative TRAP-stained cells (*red*), Ki-67-stained cells (*brown*), and cleaved caspase-3-stained cells (*brown*). The numbers of TRAP-positive cells per length of tumor-contacting bone were counted, and the percentages of Ki-67-positive cells and cleaved caspase-3-positive cells were calculated. *B,* bone. *Columns,* mean; *bars,* SD.

stimulation with 1 μmol/L PGE_2. Similar to the results in PC-3 cells, this induction was inhibited by treatment with a 3-fold dose of 293-FuEP2/Ex2 CM and this inhibition was decreased by treatment of 10 μmol/L PGE_2 (Fig. 2C).

Growth Activity of PC3-FuEP2/Ex2 Cells

To examine the effect of FuEP2/Ex2 on an osteolytic bone metastasis model *in vivo*, we attempted to establish a cell line that stably expressed FuEP2/Ex2 from PC-3 cells. By using RT-PCR and ELISA, expression of FuEP2/Ex2 mRNA and protein as well as FuEP2/Ex2 protein secretion was confirmed. Calculation of the secretion levels based on the A_{450} values revealed that the level in PC3-FuEP2/Ex2 CM was 1.59-fold when the level in the mock-transfected control CM (PC3-Fumock) was set at 1.00 (Fig. 3A). We designated this cell line PC3-FuEP2/Ex2. MTT (Fig. 3B) and colony formation (Fig. 3C) assays showed that the growth rates of PC3-Fumock and PC3-FuEP2/Ex2 cells under nonstimulated conditions were similar. Effect of PGE_2 on the growth stimulation was also tested. PGE_2 dose-dependently stimulated cell growth in PC3-Fumock, whereas no significant stimulation was observed in PC3-FuEP2/Ex2. Moreover, at both doses, growth stimulation by PGE_2 was significantly decreased in PC3-FuEP2/Ex2 cells compared with PC3-Fumock cells ($P < 0.02$ in 1 μmol/L PGE_2-treated groups and $P < 0.005$ in 10 μmol/L PGE_2-treated groups; Fig. 3D).

PC3-FuEP2/Ex2-Injected Mouse Tibias Show Decreased Osteolysis with Down-regulation of COX-2, IL-1β, and IL-6 mRNAs

A xenograft model involving by intraosseous injection of cells into the tibia of nude mice was conducted. PC3-Fumock or PC3-FuEP2Ex2 cells were injected into the bone of nude mice (10 mice for PC3-Fumock and 11 mice for PC3-FuEP2/Ex2). The osteolytic lesions were observed at 9 weeks after the injection. Radiographically, severe osteolysis was observed in all of PC3-Fumock-injected mice, whereas the bone structure was preserved in all of PC3-FuEP2/Ex2-injected mice (Fig. 4A). The FuEP2/Ex2, COX-2, IL-1β, and IL-6 mRNA expression levels in the tumors was also examined. FuEP2/Ex2 mRNA expression was only detected in the tumors in PC3-FuEP2Ex2-injected mice. The expression levels of COX-2, IL-1β, and IL-6 mRNAs in PC3-FuEP2/Ex2-injected mice were reduced compared with those in PC3-Fumock-injected mice (Fig. 4B). The average hind limb weight and incidence of intraabdominal lymph node metastases in the PC3-FuEP2Ex2-injected mice were 0.65 ± 0.06 and 18.2%, respectively, compared with 0.87 ± 0.24 and 60% in PC3-Fumock-injected mice, respectively (Table 1). Statistical analyses revealed that these reductions in PC3-FuEP2/Ex2-injected mice were significant.

Decreased Osteoclasts and Increased Apoptotic Cells in the Tumors of PC3-FuEP2/Ex2-Treated Mice

We did histologic examination to assess the number of TRAP-positive cells (osteoclasts), Ki-67-positive cells (proliferating cells), and cleaved caspase-3-positive cells (apoptotic cells) in PC3-FuEP2/Ex2- and PC3-Fumock-injected mice. The measurements were conducted in 10 fields in the tumor adjacent to the bone. The number of TRAP-positive cells per length of bone surface was significantly lower in PC3-FuEP2/Ex2-injected mice than in PC3-Fumock-injected mice (13.4 ± 6.0 in PC3-FuEP2/Ex2-injected mice versus 27.2 ± 4.8 in PC3-Fumock-injected mice; $P < 0.001$; Fig. 5A). The percentages of Ki-67-positive cells did not differ

Table 1. Tumor incidence, weight of hind legs, and lymph node metastasis of PC3-Fumock- or PC3-FuEP2/Ex2-injected mice

Injected cells	Incidence of bone tumors (%)	Average weight of hind legs (g)	Incidence of intraabdominal lymph node metastasis (%)
PC3-Fumock	100.0 (10/10)	0.87 ± 0.24	60.0 (6/10)
PC3-FuEP2/Ex2	100.0 (11/11)	0.65 ± 0.06*	18.2 (2/11)†

*Significantly different from PC3-Fumock at $P < 0.01$ by the Student's t test.
†Significantly different from PC3-Fumock at $P < 0.05$ by the χ^2 test.

significantly (52.7 ± 31.0% in PC3-FuEP2/Ex2-injected mice and 58.8 ± 20.1% in PC3-Fumock-injected mice; Fig. 5B). The percentage of cleaved caspase-3-positive cells was significantly higher in PC3-FuEP2/Ex2-injected mice than in PC3-Fumock-injected mice (11.4 ± 5.9% in PC3-FuEP2/Ex2-injected mice versus 4.9 ± 3.8% in PC3-Fumock-injected mice; $P < 0.01$; Fig. 5C).

Discussion

Recently, inhibition of EP signaling has been considered a hopeful target for antitumor, anticarcinogenic, and antimetastatic strategies. This idea has mainly arisen due to three reasons. First, the signaling of EPs and subsequent cellular events, particularly after EP2 and EP4 signaling, are known to be accelerated in a wide variety of cancers. Second, EPs are constitutively expressed in many tissues and therefore able to act as triggers of abnormal cell proliferation under conditions in which high levels of PGE_2 exist. Third, *in vivo* analyses of EP-deficient mice or antagonism of EPs clearly showed suppression of carcinogenesis, tumor growth, and metastasis (11–16). In the current study, we have shown a novel approach for EP inhibition by using a decoy EP as a specific scavenger of PGE_2.

We designed several patterns of expression vectors encoding hEP2 cDNA fragments, introduced these vectors into 293 cells, and found that 293-FuEP2/Ex2 CM exhibited specific capturing activity for PGE_2. Using point mutation assays, Stillman et al. showed previously that the PGE_2-binding activity of hEP2 required the second extracellular loop (25). Our results are consistent with that report. However, the present study is the first report that a partial fragment of the second extracellular loop of hEP2 is also able to capture PGE_2. FuEP2/Ex2 CM inhibited PGE_2-mediated phosphorylation of CREB and the subsequent induction of COX-2, IL-1β, and IL-6 mRNAs in PC-3 cells and RANKL mRNA in human osteoblasts. In all variables, exposure of excess amount of PGE_2 attenuated these inhibitions. These results suggest that the neutralization by FuEP2/Ex2 occurs in competitive manner. Induction of COX-2 by PGE_2 was reported to be regulated via EP2- or EP4-mediated signaling (26). IL-1β and IL-6 are closely related to cancer bone metastasis and are also called ''osteolytic cytokines'' (27, 28). Furthermore, these three genes have cAMP response element sites in their promoter regions and can be regulated by cellular cAMP (29–31). Moreover, The RANKL/RANK system in osteoblasts and osteoclasts is the dominant mediator of osteoclastogenesis. Thus, our findings strongly suggest that FuEP2/Ex2 will be useful as a decoy receptor for PGE_2 to prevent cancer bone metastasis.

Bone is one of the most preferential sites for metastasis of prostate cancer (32). Therefore, we used prostate cancer PC-3 cells to establish a stable transfectant expressing FuEP2/Ex2 (PC3-FuEP2/Ex2) to test whether FuEP2/Ex2 was effective in a bone metastasis model. PC-3 cells expresses EP2 and EP4, and their xenograft breaks through the bone and invades the surrounding tissue (23, 33). These characteristics were suitable to investigate whether bone lysis is obstructed by FuEP2/Ex2. PC3-FuEP2/Ex2 cells grew at the same rate as mock-transfected control cells (PC3-Fumock) *in vitro*. When stimulated with PGE_2, however, the growth rate of PC3-FuEP2/Ex2 cells was significantly slower than that of PC3-Fumock cells. PGE_2 is known to induce the proliferation of cancer cells, including PC-3 cells (34). Hence, this finding is probably due to neutralization of PGE_2 by secreted FuEP2/Ex2. PC3-FuEP2/Ex2-injected mice showed apparent reduction in hind limb weight, osteolysis, and lymph node metastasis. Furthermore, the expression levels of COX-2, IL-1β, and IL-6 mRNAs were markedly reduced. These results strongly suggest that FuEP2/Ex2 functions as a decoy receptor for PGE_2 in the same manner as in the *in vitro* experiments and that IL-1β and IL-6 play central roles in the osteolytic growth stimulation by PGE_2 in PC-3 cells.

Histologic analyses revealed that the number of osteoclasts was decreased and the percentage of apoptotic cells was increased in PC3-FuEP2/Ex2 tumors, without affecting the percentage of proliferating cells. PGE_2 is one of the stimulators of osteoclastogenesis, with induction of RANKL in osteoblasts (17, 18). Moreover, PGE_2 was reported to abolish apoptosis in some cancer cells by up-regulating antiapoptotic proteins and enhancing cell survival pathways (35, 36). However, the possibility that secreted FuEP2/Ex2 may directly induce apoptosis of cancer cells can be excluded, because the growth rate of PC3-FuEP2/Ex2 cells *in vitro* was almost the same as that of the parental cells. Furthermore, the cleaved caspase-3-positive cells were fewer in tumors grown outside of the bone than those in tumors adjacent to the bone (data not shown). Hence, these results suggest that neutralization of PGE_2 by secreted FuEP2/Ex2 directly suppresses cell differentiation into osteoclasts and that the depletion of PGE_2 was one of the reasons for the increase in apoptotic cells. In addition, induction of apoptosis by FuEP2/Ex2 may be related with a change (e.g., signaling of differentiation to the osteoclasts) of bone microenvironment rather than direct action to tumor cells.

This is the first report that a partial fragment of hEP2 containing the second extracellular loop shows potent

binding activity toward PGE_2. This activity affected PGE_2-stimulated cell signaling and tumor growth in the bones of nude mice. These findings suggest that FuEP2/Ex2 may be a useful agent for neutralizing abnormal cell events induced by excess amounts of PGE_2 as a peptide drug or a candidate for gene therapy for EP-dependent diseases as well as many types of cancers. At the present time, inhibition of individual EPs by specific antagonists has been applied to cancer therapy and prevention, because blockade of all types of prostaglandins frequently causes adverse effects, even if a specific COX-2 inhibitor is used (37, 38). However, the effects of long-term administration of specific antagonists for EPs are unknown. Compared with these antagonists, all components of FuEP2/Ex2 are of human origin. This fact suggests that FuEP2/Ex2 is unlikely to cause severe immunogenicity. Furthermore, the second extracellular region of hEP2 is only 22 amino acids in length, and this small size will be an advantage for synthesis, chemical modulation, and pharmaceutical preparation. Moreover, $PGF_{2\alpha}$ and its specific receptor FP are involved in angiogenesis, motility, and invasion in cancer in a similar manner to PGE_2 (39, 40). By using a similar approach to the one described in this report, it may be possible to generate an effective neutralizing agent for $PGF_{2\alpha}$ that has the same advantages as FuEP2/Ex2.

In conclusion, we have shown that FuEP2/Ex2 has capturing activity for PGE_2 and can inhibit PGE_2-induced cell signaling *in vitro*. Moreover, FuEP2/Ex2 reduced the degrees of tumor growth and osteolysis in a xenograft model of bone metastasis. Our data strongly suggest that FuEP2/Ex2 will be a promising agent for PGE_2-dependent cancers, especially with regard to osteolytic bone metastasis.

Disclosure of Potential Conflicts of Interest

No potential conflicts of interest were disclosed.

Acknowledgments

We thank Dr. Saburo Sone (Department of Internal Medicine and Molecular Therapeutics, University of Tokushima School of Medicine) for providing the human osteoblasts and Megumi Satoh and Hitomi Umemoto for technical assistance.

References

1. Wang D, Dubois RN. Prostaglandins and cancer. Gut 2006;55:115 – 22.

2. Ono K, Akatsu T, Murakami T, et al. Involvement of cyclo-oxygenase-2 in osteoclast formation and bone destruction in bone metastasis of mammary carcinoma cell lines. J Bone Miner Res 2002;17:774 – 81.

3. Gamradt SC, Feeley BT, Liu NQ, et al. The effect of cyclooxygenase-2 (COX-2) inhibition on human prostate cancer induced osteoblastic and osteolytic lesions in bone. Anticancer Res 2005;25:107 – 15.

4. Singh B, Berry JA, Shoher A, Ayers GD, Wei C, Lucci A. COX-2 involvement in breast cancer metastasis to bone. Oncogene 2007;26: 3789 – 96.

5. Coleman RA, Smith WL, Narumiya S. International Union of Pharmacology classification of prostanoid receptors: properties, distribution, and structure of the receptors and their subtypes. Pharmacol Rev 1994;46: 205 – 29.

6. Funk CD, Furci L, FitzGerald GA, et al. Cloning and expression of a cDNA for the human prostaglandin E receptor EP1 subtype. J Biol Chem 1993;268:26767 – 72.

7. Bastien L, Sawyer N, Grygorczyk R, Metters KM, Adam M. Cloning, functional expression, and characterization of the human prostaglandin E_2 receptor EP2 subtype. J Biol Chem 1994;269:11873 – 7.

8. Namba T, Sugimoto Y, Negishi M, et al. Alternative splicing of C-terminal tail of prostaglandin E receptor subtype EP3 determines G-protein specificity. Nature 1993;365:166 – 70.

9. Regan JW, Bailey TJ, Pepperl DJ, et al. Cloning of a novel human prostaglandin receptor with characteristics of the pharmacologically defined EP2 subtype. Mol Pharmacol 1994;46:213 – 20.

10. Siu YT, Jin DY. CREB-a real culprit in oncogenesis. FEBS J 2007;274: 3224 – 32.

11. Watanabe K, Kawamori T, Nakatsugi S, et al. Role of the prostaglandin E receptor subtype EP1 in colon carcinogenesis. Cancer Res 1999;59:5093 – 6.

12. Mutoh M, Watanabe K, Kitamura T, et al. Involvement of prostaglandin E receptor subtype EP_4 in colon carcinogenesis. Cancer Res 2002;62: 28 – 32.

13. Sonoshita M, Takaku K, Sasaki N, et al. Acceleration of intestinal polyposis through prostaglandin receptor EP2 in Apc (Δ716) knockout mice. Nat Med 2001;7:1048 – 51.

14. Kitamura T, Itoh M, Noda T, et al. Combined effects of prostaglandin E receptor subtype EP1 and subtype EP4 antagonists on intestinal tumorigenesis in adenomatous polyposis coli gene knockout mice. Cancer Sci 2003;94:618 – 21.

15. Niho N, Mutoh M, Kitamura T, et al. Suppression of azoxymethane-induced colon cancer development in rats by a prostaglandin E receptor EP1-selective antagonist. Cancer Sci 2005;96:260 – 4.

16. Yang L, Huang Y, Porta R, et al. Host and direct antitumor effects and profound reduction in tumor metastasis with selective EP4 receptor antagonism. Cancer Res 2006;66:9665 – 72.

17. Ohshiba T, Miyaura C, Ito A. Role of prostaglandin E produced by osteoblasts in osteolysis due to bone metastasis. Biochem Biophys Res Commun 2003;300:957 – 64.

18. Liu XH, Kirschenbaum A, Yao S, Levine AC. Cross-talk between the interleukin-6 and prostaglandin E_2 signaling systems results in enhancement of osteoclastogenesis through effects on the osteoprotegerin/receptor activator of nuclear factor-κB (RANK) ligand/RANK system. Endocrinology 2005;146:1991 – 8.

19. Fuller K, Wong B, Fox S, Choi Y, Chambers TJ. TRANCE is necessary and sufficient for osteoblast-mediated activation of bone resorption in osteoclasts. J Exp Med 1998;188:997 – 1001.

20. Miyaura C, Inada M, Suzawa T, et al. Impaired bone resorption to prostaglandin E_2 in prostaglandin E receptor EP4-knockout mice. J Biol Chem 2000;275:19819 – 23.

21. Sabino MA, Ghilardi JR, Jongen JL, et al. Simultaneous reduction in cancer pain, bone destruction, and tumor growth by selective inhibition of cyclooxygenase-2. Cancer Res 2002;62:7343 – 9.

22. Takita M, Inada M, Maruyama T, Miyaura C. Prostaglandin E receptor EP4 antagonist suppresses osteolysis due to bone metastasis of mouse malignant melanoma cells. FEBS Lett 2007;581:565 – 71.

23. Chen Y, Hughes-Fulford M. Prostaglandin E_2 and the protein kinase A pathway mediate arachidonic acid induction of c-fos in human prostate cancer cells. Br J Cancer 2000;82:2000 – 6.

24. Uehara H, Kim SJ, Karashima T, et al. Effects of blocking platelet-derived growth factor-receptor signaling in a mouse model of experimental prostate cancer bone metastases. J Natl Cancer Inst 2003;95:558 – 70.

25. Stillman BA, Audoly L, Breyer RM. A conserved threonine in the second extracellular loop of the human EP2 and EP4 receptors is required for ligand binding. Eur J Pharmacol 1998;357:73 – 82.

26. Bradbury DA, Newton R, Zhu YM, El-Haroun H, Corbett L, Knox AJ. Cyclooxygenase-2 induction by bradykinin in human pulmonary artery smooth muscle cells is mediated by the cyclic AMP response element through a novel autocrine loop involving endogenous prostaglandin E_2, E-prostanoid 2 (EP2), and EP4 receptors. J Biol Chem 2003;278:49954 – 64.

27. Anasagasti MJ, Olaso E, Calvo F, et al. Interleukin 1-dependent and -independent mouse melanoma metastasis. J Natl Cancer Inst 1997;89: 645 – 51.

28. Kurihara N, Bertolini D, Suda T, Akiyama Y, Roodman GD. IL-6

stimulates osteoclast-like multinucleated cell formation in long term human marrow cultures by inducing IL-1 release. J Immunol 1990;144: 4226 – 30.

29. Inoue H, Yokoyama C, Hara S, Tone Y, Tanabe T. Transcriptional regulation of human prostaglandin-endoperoxide synthase-2 gene by lipopolysaccharide and phorbol ester in vascular endothelial cells. Involvement of both nuclear factor for interleukin-6 expression site and cAMP response element. J Biol Chem 1995;270:24965 – 71.

30. Gray JG, Chandra G, Clay WC, et al. A CRE/ATF-like site in the upstream regulatory sequence of the human interleukin 1β gene us necessary for induction in U937 and THP-1 monocytic cell lines. Mol Cell Biol 1993;13:6678 – 89.

31. Ray A, Sassone-Corsi P, Sehgal PB. A multiple cytokine- and second messenger-responsive element in the enhancer of the human interleukin-6 gene: similarities with c-fos gene regulation. Mol Cell Biol 1989;9: 5537 – 47.

32. DeAntoni EP, Crawford ED. Pretreatment of metastatic disease. Prostate cancer in the older male. Cancer 1994;74:2182 – 7.

33. Soos G, Jones RF, Haas GP, Wang CY. Comparative intraosseal growth of human prostate cancer cell lines LNCaP and PC-3 in the nude mouse. Anticancer Res 1997;17:4253 – 8.

34. Tjandrawinata RR, Hughes-Fulford M. Up-regulation of cyclooxygenase-2 by product-prostaglandin E_2. Adv Exp Med Biol 1997;407: 163 – 70.

35. Sheng H, Shao J, Morrow JD, Beauchamp RD, Dubois RN. Modulation of apoptosis and bcl-2 expression by prostaglandin E_2 in human colon cancer cells. Cancer Res 1998;58:362 – 6.

36. George RJ, Sturmoski MA, Anant S, Houchen CW. EP4 mediates PGE_2 dependent cell survival thorough the PI3 kinase/AKT pathway. Prostaglandins Other Lipid Mediat 2007;83:112 – 20.

37. Ray WA, Stein CM, Daugherty JR, Hall K, Arbogast PG, Griffin MR. COX-2 selective non-steroidal anti-inflammatory drugs and risk of serious coronary heart disease. Lancet 2002;360:1071 – 3.

38. Fitzgerald GA. Coxibs and cardiovascular disease. N Engl J Med 2004;351:1709 – 11.

39. Sales KJ, List T, Boddy SC, et al. A novel angiogenic role for prostaglandin $F_{2\alpha}$-FP receptor interaction in human endometrial adenocarcinomas. Cancer Res 2005;65:7707 – 16.

40. Qualtrough D, Kaidi A, Chell S, Jabbour HN, Williams AC, Paraskeva C. Prostaglandin $F_{2\alpha}$ stimulates motility and invasion in colorectal tumor cells. Int J Cancer 2007;121:734 – 40.